Available online at www.sciencedirect.com

ScienceDirect

Procedia Materials Science 8 (2015) 1118 – 1126

Procedia Materials Science

www.elsevier.com/locate/procedia

International Congress of Science and Technology of Metallurgy and Materials, SAM - CONAMET 2013

Evaluation of the Abnormal Grain Growth in an ASTM 213 Grade T91 Steel.

J.L. Gibson[a], C. Jiménez[b], C. García de Andrés[c], C.A. Danón[d], M.I. Luppo[d]*

[a]*Instituto Sabato-UNSAM/CNEA, Av. Gral Paz 1499 (B1650KNA) San Martín, Buenos Aires, Argentina*
[b]*Helmholtz-Zentrum Berlin, Albert-Einstein-Strasse 15, 12489 Berlín, Alemania*
[c]*Grupo de Investigación MATERIALIA,CENIM-CSIC, Av. Gregorio del Amo 8, Madrid,España*
[d]*Gerencia Materiales, GAEN, CNEA, Av. Gral Paz 1499 (B1650KNA) San Martín, Buenos Aires, Argentina*

Abstract

A study of the austenite grain growth of an ASTM A213 T91 steel held at 1050ºC for increasing times is presented. The prior austenite grain size distribution (PAGSD) at various holding times was determined using scanning electron microscopy. Taking into account the critical role played by MX precipitates (M: metal, X: C and/or N) on grain growth, transmission electron microscopy on replicas was used to characterize the carbides or carbonitrides present during holding in austenite; thus, the particle size distribution and chemical composition of these precipitates were determined for each austenite holding time. Results indicate a change in the chemical identity of the MX precipitates –from V-rich to Nb-rich- during the first minutes of austenite holding, the $M_{23}C_6$ dissolution and the further austenite grain growth in a heterogeneous mode.

Selection and peer-review under responsibility of the scientific committee of SAM - CONAMET 2013

Keywords: Ferritic-martensitic steels; grain growth, electron microscopy; microstructure; X-ray diffraction.

1. Introduction

Ferritic-martensitic steels of the 9%Cr1%Mo type have been extensively used in conventional and nuclear power plant components, heat exchangers, piping and tubing, etc., due to an excellent combination of properties such us creep resistance, toughness and resistance to oxidation at high temperatures (Fujita (1992); Masuyama, (2001);

* Corresponding author. Tel.: +057-11-6772-7499; fax: +057-11-6772-7763.
*E-mail address:*luppo@cnea.gov.ar

Selection and peer-review under responsibility of the scientific committee of SAM - CONAMET 2013
doi:10.1016/j.mspro.2015.04.175

Klueh, (2005)). Over the last two decades, these steels were considered as main candidates for manufacturing structural components in Generation IV nuclear reactors because they have excellent irradiation resistance to void swelling (Klueh and Nelson (2007)).The 9%Cr1%Mo steels in the normalized and tempered metallurgical state show a martensitic matrix with a high dislocation density and $M_{23}C_6$precipitated carbides (M is primarily Cr, Fe, and Mo). If V and Nb are present in the composition (for instance, in the T91 steel), there will be also a fine distribution of small MX (M is primarily Nb and V, and X is C and N) vanadium and/or niobium carbonitrides (Klueh (2005)). The austenite grain boundaries and dislocations are pinned by the precipitates, inhibiting their movement during the thermomechanical processing of steels. The pinning force is governed by the thermodynamic stability of second phase precipitates in austenite (Gladman and Pickering (1967)). If austenite holding is carried out above a certain temperature the driving force for grain growth will be higher than the pinning force, abnormal grain growth will begin and a non-uniform grain microstructure will be obtained, which degrades the mechanical properties of these materials (Chakrabarti et al. (2009); Kundu et al. (2011)).

The influence of the heating rate to austenite on the austenite grain size distribution has been reported in the literature referred to carbon steels (Sheard and Nutting ((1979)), microalloyed steels containing Ti and V (Peñalba et al. (1996)) or Nb (Rossi et al. (1987)), and martensitic steels (Danón et al.(2003)). Studies carried out in each case have allowed to establish that there is a complex dependence of the austenite grain size distribution with respect to the austenitization conditions (austenitization temperature and holding time, heating rate to austenite) and the initial metallurgical state of the material. Thus, by varying the heating rate without changing the austenitization temperature and holding time, two types of austenite grain structure –i.e. homogeneous or heterogeneous- could be obtained.

In a previous work (Zavaleta Gutiérrez et al. in press)it was reported that samples of an ASTM A213 T91 steel held at 1050°C for 30 minutes showed only heterogeneous grain growth after being heated to austenite at a rate of 50°C s^{-1}. However, heating at rates high enough is a necessary but not sufficient condition for the occurrence of such a heterogeneous grain growth. The absence of abnormal grain growth in the Nb and V-free T9 steel demonstrates that the MX precipitates play a major role in the heterogeneous austenite grain growth phenomenon. On the basis of these results a study of the microstructural evolution of the T91 steel for intermediate holding times in austenite was proposed, in order to clarify the time for triggering the heterogeneous grain growth during austenitization.

In the present work the grain growth of an ASTM A213 T91 steel held at 1050°C is analyzed and, in particular, the prior austenite grain size distributions (PAGSD's) for increasing times at that temperature are determined. Taking into account the critical role played by the second phase particles, the particle size distribution and the chemical composition of the Nb and V carbonitrides for each austenite holding time at 1050°C are also obtained.

2. Experimental Procedure

Samples for the thermal cycles – cylinderd 12 mm in length and 3 mm in diameter – were machined following the rolling direction of a tube (8mm wall thickness) provided by Vallourec & Mannesmann (France). The material was received in its standard condition, that is, normalized at 1060 °C and tempered 40 minutes at 780 °C. The certified chemical composition for this material is shown in Table 1.

Table 1. Chemical composition of the P91 steel in wt%.

C	Cr	Mo	Si	V	Nb	N	Mn	Ni	Al
0.11	8.28	0.93	0.28	0.21	0.07	0.045	0.48	0.11	0.015

The thermal cycles were carried out in the heating and cooling devices of an Adamel Lhomargy DT1000 high speed, high-resolution dilatometer. Samples were heated to 1050 °C at 50 °C s^{-1}, held at that temperature for increasing times and then quenched at 50 °C s^{-1} to room temperature applying a cold He jet. The various holding times in austenite at 1050 °C are described in Table 2.

Table 2: Thermal cycles carried out in the Adamel DT1000 dilatometer and holding times at 1050 ºC.

Test	$t_{1050ºC}$ (min)
S0	0
S5	5
S10	10
S20	20
S40	40

Samples were cross-cut through by the mid-plane so as to obtain two identical pieces. One half was used to study the present particles by means of electron microscopy and X-ray diffraction with synchrotron light. The other half underwent a second tempering treatment at the usual industrial temperature (780 °C) during 30 minutes so as to highlight the prior austenite grain boundaries by precipitation of $M_{23}C_6$ carbide particles. In this way, a better visualization of the grain boundaries was achieved. Then, samples were embedded in a resin, grounded so as to expose the mid plane, polished down to 1 μm diamond cloth and etched with the Villela reagent.

The PAGSD of each sample was determined by automatic image analysis performed with a commercial software package on the images acquired in a scanning electron microscope (SEM) FEI Quanta 200. Approximately 450 to 1500 grains were counted in each sample. Prior austenite grain size number frequency histograms were constructed, using a bin size of 2.5 μm in all cases.

The study of the particle size and chemical composition was carried out in a transmission electron microscope (TEM) Phillips CM200 attached with an EDAX-DX4 system for energy dispersive analysis of X-rays (EDS) in carbon replicas extracted of each sample. From these measurements, number frequency histograms for the particle size were constructed; in this case, the optimum bin size was chosen in agreement with the Wand criterion (Wand(1997)).The distribution of precipitates in the matrix was observed by means of a scanning electron microscope with field emission gun (FEG-SEM) Zeiss Supra-40.

Preliminary results for the characterization of samples by means of the ED-XRD technique (Energy-Dispersive X-Ray Diffraction) in the EDDI (Energy Dispersive Diffraction) experimental station at the BESSY II synchrotron light source of the Helmholtz Centre Berlin (Genzel et al. (2007)) are also shown. Samples were illuminated by an X-ray polychromatic beam and diffracted spectra were measured in the energy-dispersive mode using the Bragg-Brentano reflection geometry at $2\theta = 7º$ by a multichannel analyzing detector. The energy range was between 30 and 90 keV, where the detector efficiency is higher.

3. Results

3.1. Prior austenite grain size distributions (PAGSD's)

Fig. 1 shows the prior austenite grain size number frequency histograms and Table 3 the statistical parameters corresponding to each grain size distribution. Heterogeneous grain growth was observed only in the sample austenitized during 40 minutes (S40).

Even though in the S0 sample homogeneous grain growth was observed, it was very difficult to define prior austenite grain boundaries from the SEM micrographs, probably because the additional heat treatment to decorate these boundaries did not induce additional precipitation of $M_{23}C_6$ carbides over that already present in the sample before the thermal treatment (see 3.2). In the rest of the samples, the mean grain size remains constant as a function of the austenite holding time and the same happens with the other statistical parameters that characterize the distributions. The only exception seems to be the kurtosis coefficient, which increases for the sample austenitized for 40 minutes. Such increment does not have correlation with the presence of large grains in this sample, which were excluded of the calculation with the aim of comparing similar populations.

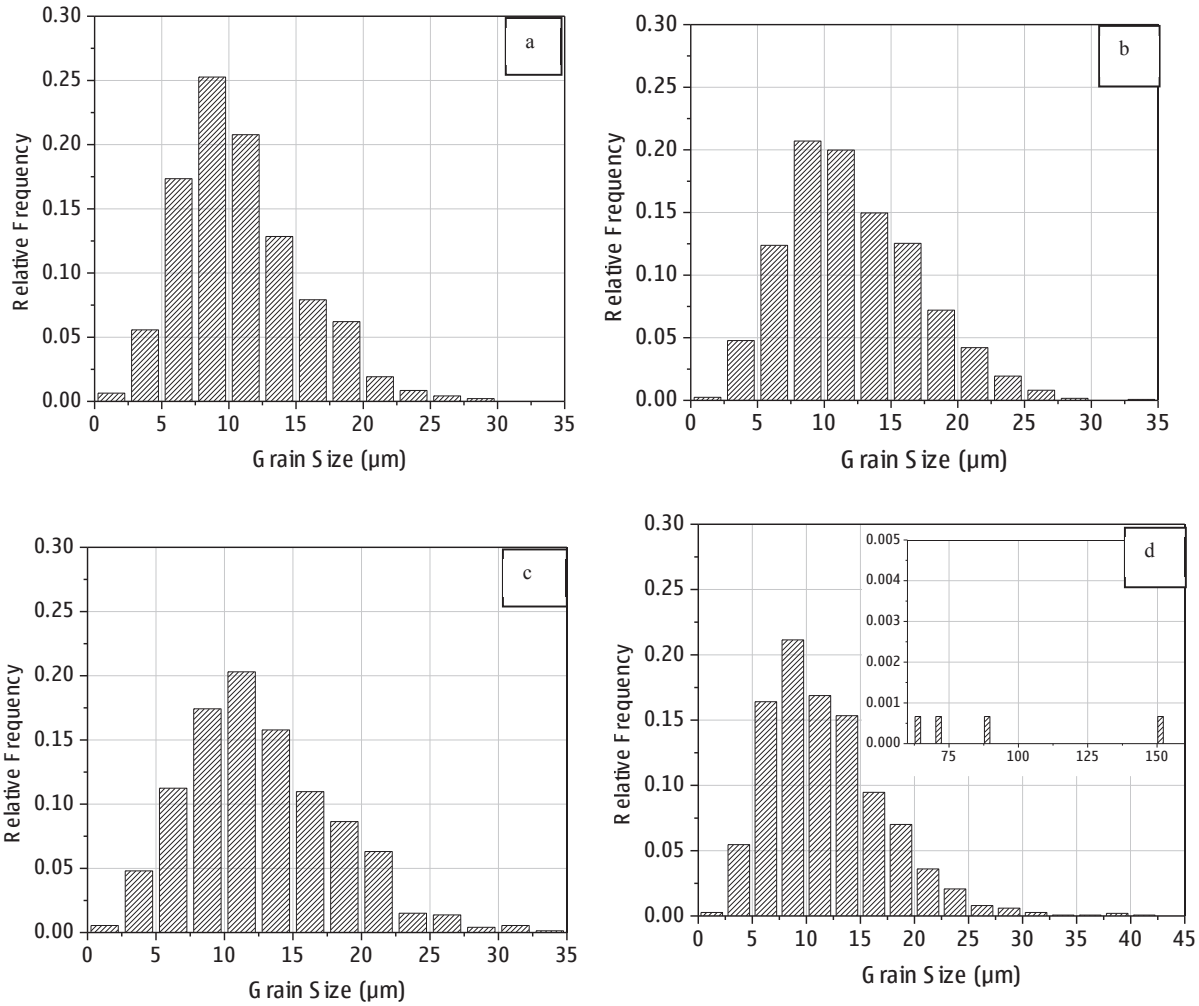

Fig. 1. Prior austenite grain size number frequency histograms for the studied samples.

Table 3. Statistical parameters of the prior austenite grain size distributions.

Sample	Statistical Parameter					
	N	Mean Size (μm)	Standard Deviation (μm)	Assymetry Coefficient	Kurtosis Coefficient	Variation Coefficient
S5	467	10.8	4.5	0.74	0.48	0.42
S10	1236	12.1	4.9	0.60	0.20	0.41
S20	729	12.7	5.5	0.67	0.4	0.43
S40	1491	11.8	5.3	0.88	0.93	0.45

3.2. Characterization of the second phases precipitated by means of electron microscopy

The study of the precipitated phases in the as-received metallurgical state was reported in a previous work (Zavaleta Gutiérrez et al. (2011)). The $M_{23}C_6$ carbide phase was the major observed phase (mean particle size: 141 nm; chemical composition: 58%Cr-32.3%Fe-8.4%Mo-1.4%V; morphology: varied). The next precipitated phases as for the estimated volume fraction were, in descending order: MX type II or VN (mean particle size: 51 nm; chemical composition: 67.5%V-11.8%Nb-21.1%Cr; morphology: plate or rod), MX type III or "wings" (in which MX type II rods, ellipsoids or plates grow after nucleating on the sides of a MX type I spherical core), MX type I or NbCN (mean particle size: 34 nm; chemical composition: 81.5%Nb-12.7%V-5.8%Cr, morphology: spherical), and finally complex MX or NbTiCN (particle size > 40 nm, chemical composition: similar to MX type I with Ti).

Fig. 2 shows two TEM micrographs of the S0 sample in which the identified particles are indicated by arrows. In this sample the identified precipitates were the same already present in the as-received metallurgical state, with similar chemical compositions. The $M_{23}C_6$ was still the major observed phase, followed by the MX's phases in the same order they appear in the as-received metallurgical state.

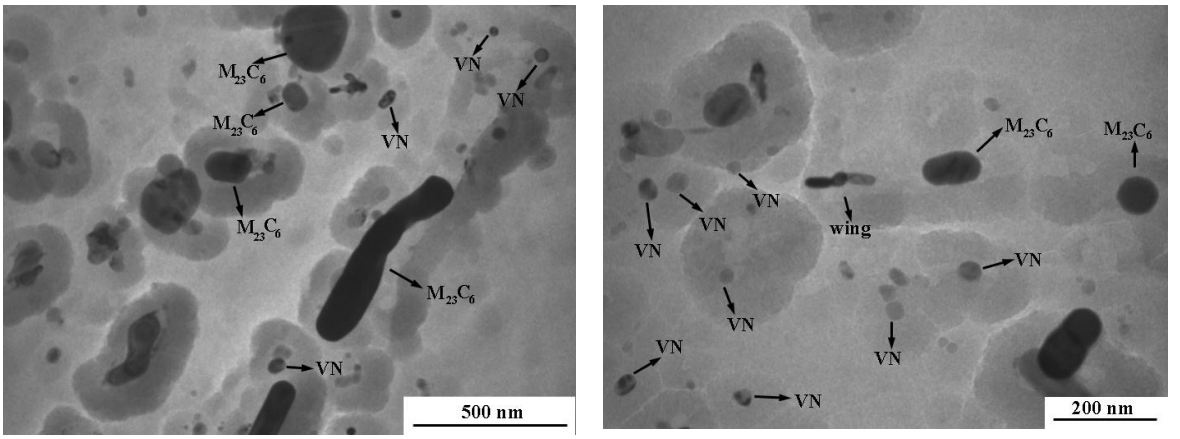

Fig. 2. TEM micrographs of extraction replicas of the S0 sample.

After 5 minutes of austenite holding at 1050 °C (samples S5, S10, S20 and S40) samples showed the MX type I as the major precipitated phase, with the same chemical composition determined for the as-received metallurgical state. In Fig. 3 a TEM micrograph corresponding to sample S40 is shown. Fig. 4 shows the particle size number frequency histograms for the MX type I precipitates. From these histograms the size evolution of the mentioned carbonitrides with the austenite holding time was obtained; it is shown in Table 4.

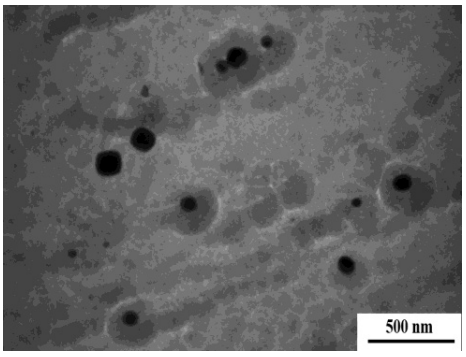

Fig. 3. TEM micrograph of an extraction replica of the S40 sample.

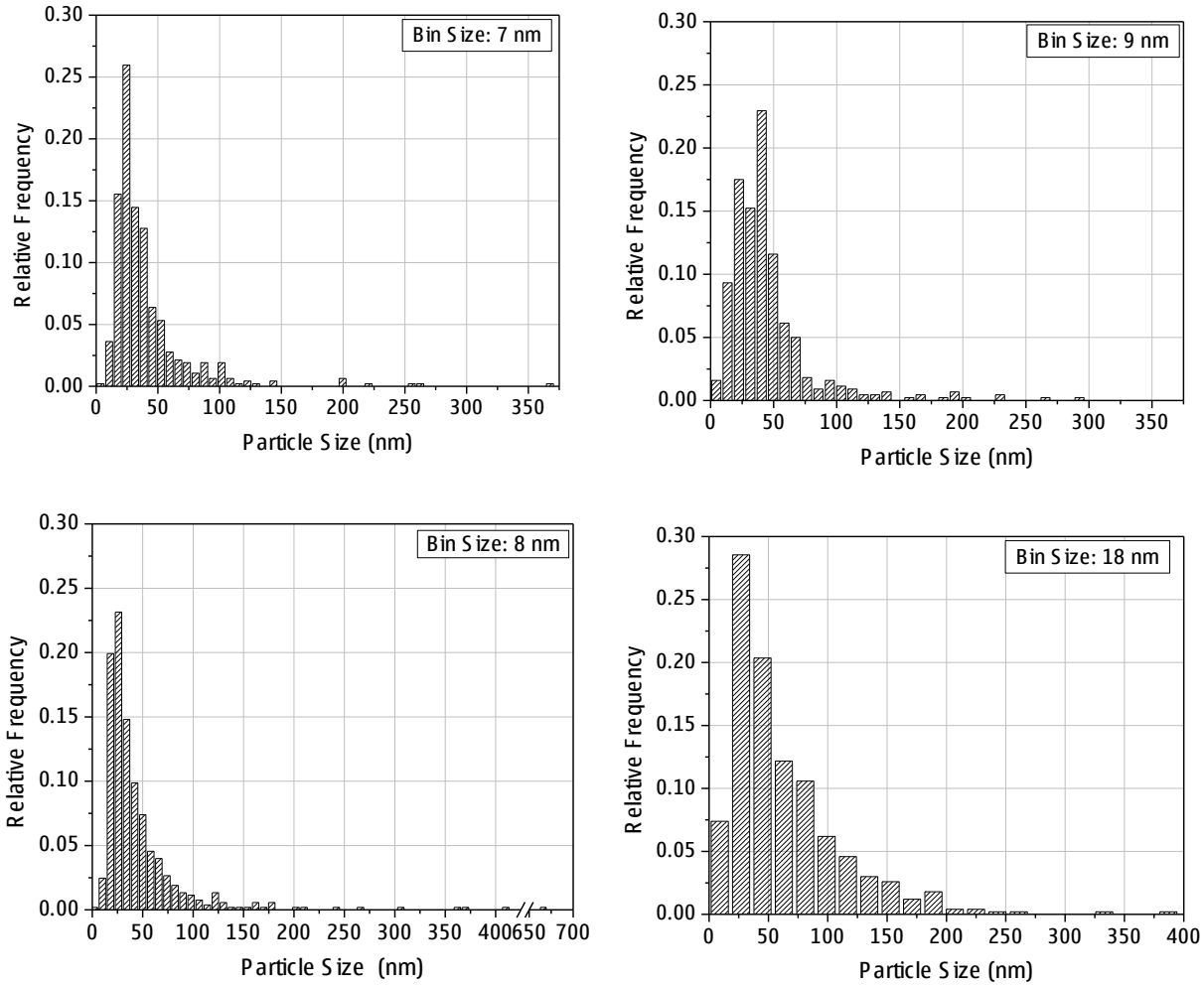

Fig. 4. Particle size number frequency histograms for the MX type I precipitate.

Table 4. Statistical parameters of the MX type I precipitates, in nanometers.

Sample	Parameter			
	N	Mean Size	Standard Deviation	Standard error of the mean
S5	470	40	35	1.6
S10	440	46	36	1.7
S20	527	46	51	2.2
S40	499	62	45	2

The minor precipitates –in a very low proportion – found in the samples austenitized from 5 minutes up were complex MX and particle agglomerates (Fig. 5) whose diffraction pattern and chemical composition coincide with the MX type I precipitate.

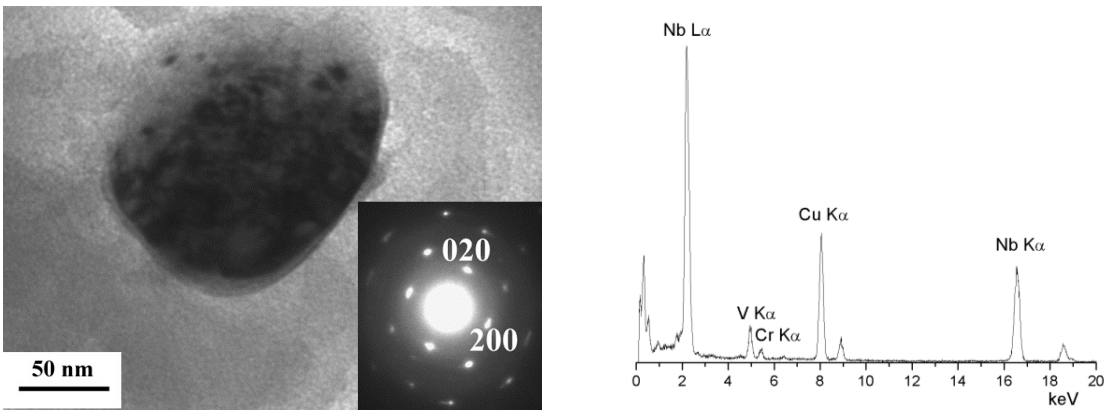

Fig. 5. TEM micrograph of an agglomerate with its corresponding diffraction pattern (axis zone z= [001]) and EDS spectrum.

Figure 6 shows FEG-SEM micrographs of the S0 and S40 samples that allow to appreciate the distribution of the precipitates in the matrix.

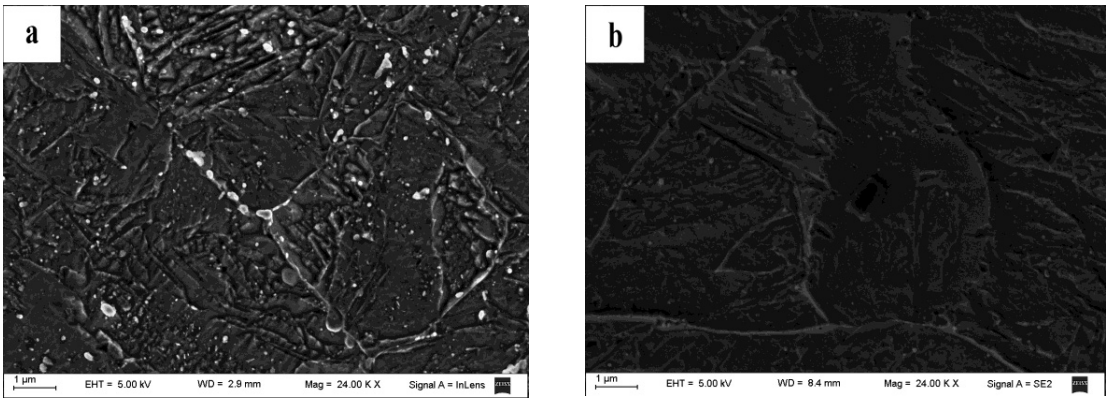

Fig. 6. FEG-SEM micrographs of a) S0 and b)S40 samples.

3.3. Characterization of the second phases precipitated by means ofX-ray diffraction with synchrotron light

Fig. 7 shows the first results obtained by means of synchrotron light based on the ED-XRD technique. In all spectra fluorescence lines of various elements (for instance, Pb $K\alpha_2$ at 72.80 keV; Pb $K\alpha_1$ at 74,97 keV) that come from the optics of the diffractometer can be seen; the escape peak of the the (110) line corresponding to the martensitic matrix is also readily distinguishable. Only in the spectrum of the sample S0 lines corresponding to the $M_{23}C_6$ precipitates were observed, but in no case it was possible to recognize the presence of MX precipitates.

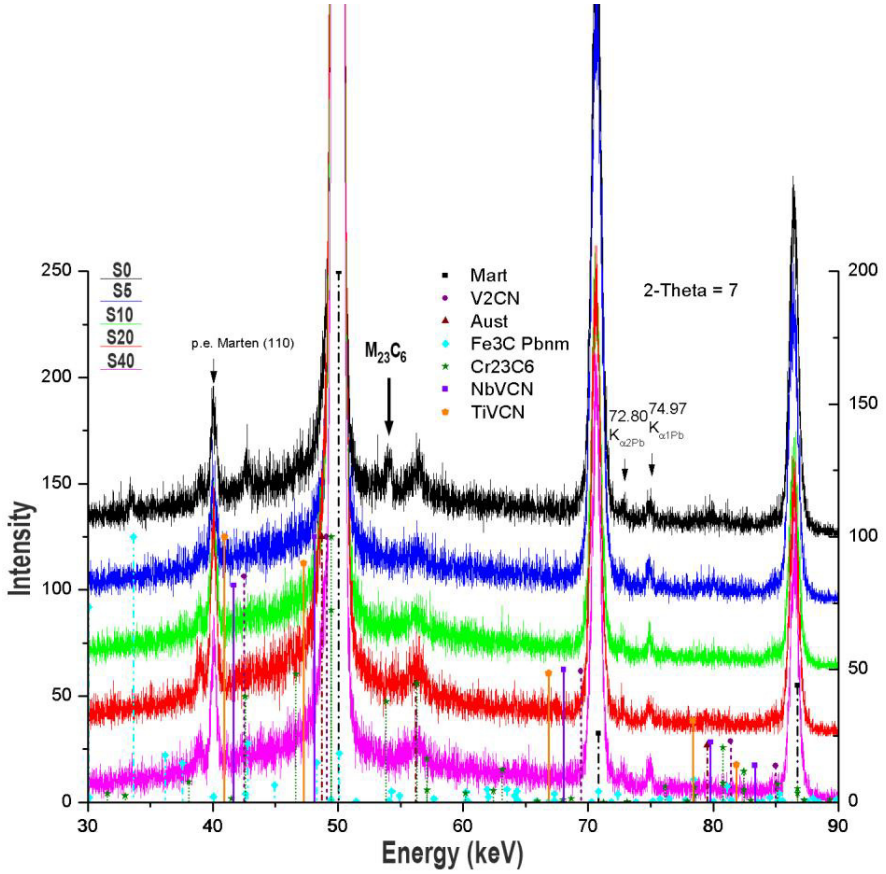

Fig. 7. ED-XRD diffraction spectrum of the samples

4. Discussion

The study of the prior austenite grain size distribution in samples heated at 50 ºC/s with increasing holding time showed heterogeneous grain growth only in the sample held at 1050 ºC during 40 minutes. On the other hand, in a previous work (Zavaleta Gutiérrez et al., in press) samples heated to austenite in the same conditions showed a heterogeneous grain size distribution after 30 minutes austenite holding time; this indicates that abnormal grain growth begins at some point between 20 and 30 minutes of holding at 1050 ºC.

In the mentioned work (Zavaleta Gutiérrez et al., in press)the change of the equilibrium fraction of precipitates with increasing temperature from 780 ºC was estimated by means of thermodynamic equilibrium calculations based on the T91 steel composition. According with these calculations (Fig. 12 in reference Zavaleta Gutiérrez et al., in press) the isothermal equilibrium dissolution of $M_{23}C_6$ is completed at ~ 900ºC, while the complete dissolution of MX occurs at ~ 1160 ºC. When the T91 steel is heated at a high rate (50 ºC/s), the dissolution of the precipitates is deferred to temperatures higher than those predicted by equilibrium conditions. The analysis of the second phase particles in each sample showed that all precipitates present in the as-received metallurgical state still remain in the material at the very beginning of austenitization, and that in the first 5 minutes of austenite holding at 1050 ºC they dissolve and/or transform predominantly in MX type I, i.e. Nb carbonitrides. These precipitates – a minor group in the as-received metallurgical state- probably nucleate and grow in the austenitization at 1050 ºC by combining the available Nb with the C released by dissolution of $M_{23}C_6$ precipitates. Moreover, they could be also formed from MX type II and III, that contain non-negligible Nb amounts and release V during the first 5 minutes of the austenite holding.

The precipitation of MX type I could occur late during the austenitization at 1050 ºC (MX type I precipitates constitute a minor fraction at the beginning of the austenite transformation) and/or it could be locally insufficient to pin efficiently austenite grains that nucleate and grow in presence of all the precipitates ($M_{23}C_6$, MX). These would be the reasons why some austenite grains grow exaggeratedly and a non-uniform grain microstructure is obtained in the T91 steel.

On the other hand, in the case of the Nb and V-free T9 steel MX type carbonitrides will be absent at all and only $M_{23}C_6$ carbides will be available at the beginning of the austenitization to pin the new austenite grains. Due to the dissolution of these precipitates in the first 5 minutes of austenite holding at 1050 ºC, austenite grains will grow uniformly and a homogeneous distribution -with a mean grain size larger than the one observed for the T91 steel- will be obtained (Zavaleta Gutiérrez et al., in press).

5. Conclusions

From the analysis of the microstructural evolution of a T91 steel heated to austenite at 50 ºC s^{-1} and held at 1050 ºC for increasing times it can be concluded that:

- Heterogeneous grain growth begins at some point between 20 and 30 minutes of holding at 1050 ºC.
- At the beginning of the austenitization, all precipitates present in the as-received metallurgical state still remain in the material.
- $M_{23}C_6$ dissolution and a change in the chemical identity of the MX precipitates (from major V-rich to major Nb-rich) occur during the first 5 minutes of austenite holding at 1050 ºC.

References

Chakrabarti, D., Davis, C.L., Strangwood, M., 2009. Effect of Deformation and Nb Segregation on Grain Size Bimodality in HSLA steel. Materials Science and Technology 25, 939-946.

Danón, A., Servant, C., Alamo, A., Brachet, J.C., 2003. "Heterogeneous Austenite Grain Growth in 9Cr Martensitic Steel: Influence of the Heating Rate and the Austenitization Temperature. Materials Science and Engineering A 348, 122-132.

Fujita, T., 1992. Current Progress in Advanced High Cr Ferritic Steels for High-Temperature Applications. ISIJ International 32, 175-181.

Genzel, Ch., Denks, I., Gibmeier, J., Klauss, M., Wagener, G., 2007. The Materials Science Synchrotron Beamline EDDI for Energy-Dispersive Diffraction Analysis. Nuclear Instruments and Methods in Physics Research A 578, 23-33.

Gladman, T., Pickering, F.B., 1967. Grain Coarsening of Austenite. Journal of the Iron and Steel Institute 205, 653-664.

Klueh,R.L., 2005. Elevated-Temperature Ferritic and Martensitic Steels and their Application to Future Nuclear Reactors. International Materials Review 50, 287-310.

Klueh, R.L., Nelson, A.T., 2007. Ferritic/Martensitic Steels for Next-Generation Reactors. Journal of Nuclear Materials 371, 37-52.

Kundu, A., Davis, C.L., Strangwood, M., 2011. Pinning of Austenite Grain Boundaries by Mixed AlN and NbCN Precipitates. Solid State Phenomena 172-174, 458-463.

Masuyama, F., 2001. History of Power Plants and Progress in Heat Resistant Steels. ISIJ International 41, 612-625.

Peñalba, F., García de Andrés, C., Carsi, M., Zapirain, F., 1996. Austenite Grain Size Evolution and Continuous Cooling Transformation Diagrams in Vanadium and Titanium Microalloyed Steels. Journal of Materials Science 31, 3847-3852.

Rosi, A., Mascanzoni, G., Crispoldi, G., de Meo, F., 1987. Development of a Nb-Ti-N Steel for Production of Tractor Links by Hot Forging and Direct Quenching. Proceedings of Fundamentals of Microalloying Forging Steels, 351-366.

Sheard, G., Nutting, J., 1979. Examination of Recrystallization and Grain Growth of Austenite with Photoemission Electron Microscopy. Metal Science 13, 131-135.

Wand, M.P., 1997. Data-Based Choice of Histogram Bin Width. The American Statistician 51, 59-64.

Zavaleta Gutiérrez, N., De Cicco, H., Marrero, J., Danón, C.A., Luppo, M.I., 2011. Evolution of Precipitated Phases During Prolonged Tempering in a 9%Cr1%MoVNb Ferritic-Martensitic Steel: Influence on Creep Performance. Materials Science and Engineering A 528, 4019-4029.

Zavaleta Gutiérrez, N. Luppo, M.I., Danón, C.A., Toda-Carvallo, I., Capdevila, C., García de Andrés, C., in press. "Heterogeneous Austenite Grain Growth in Martensitic 9Cr Steel: Coupled Influence of Initial Metallurgical State and Heating Rate. Materials Science and Technology, in press.